

Tumorigenesis and Neoplastic Progression

# Epigenetic Reversion of Breast Carcinoma Phenotype Is Accompanied by Changes in DNA Sequestration as Measured by *AluI* Restriction Enzyme

Tone Sandal,\* Klara Valyi-Nagy,\*  
Virginia A. Spencer,<sup>†</sup> Robert Folberg,\*  
Mina J. Bissell,<sup>†</sup> and Andrew J. Maniotis\*

From the Department of Pathology,\* University of Illinois at Chicago, Chicago, Illinois; and the Lawrence Berkeley National Laboratory Life Sciences Division,<sup>†</sup> Berkeley, California

**The importance of microenvironment and context in regulation of tissue-specific genes is well established. DNA exposure to or the sequestration from nucleases detects differences in higher order chromatin structure in intact cells without disturbing cellular or tissue architecture. To investigate the relationship between chromatin organization and tumor phenotype, we used an established three-dimensional assay in which normal and malignant human breast cells can be easily distinguished by the morphology of the structures they make (acinus-like versus tumor-like, respectively). We show that these phenotypes can be distinguished also by sensitivity to *AluI* digestion in which the malignant cells resist digestion relative to nonmalignant cells. Treatment of T4-2 breast cancer cells in three-dimensional culture with cAMP analogs or a phosphatidylinositol 3-kinase inhibitor not only reverted their phenotype from nonpolar to polar acinar-like structures but also enhanced chromatin sensitivity to *AluI*. By using different cAMP analogs, we show that cAMP-induced phenotypic reversion, polarization, and shift in DNA organization act through a cAMP-dependent protein-kinase A-coupled signaling pathway. Importantly, inhibitory antibody to fibronectin produced the same effect. These experiments underscore the concept that modifying the tumor microenvironment can alter the organization of tumor cells and demonstrate that architecture and global chromatin organization are coupled and highly plastic. (Am J Pathol 2007, 170:1739–1749; DOI: 10.2353/ajpath.2007.060922)**

We have shown previously that the degree of malignancy, the organization of the cytoskeleton, and the composition of the extracellular matrix (ECM) influence chromatin structure.<sup>1</sup> We found that the DNA of cultured cell lines from malignant tumors, transformed fibroblasts harboring three oncogenes, and cells collected from human malignant tumors were more resistant to nucleases compared with DNA from normal or nonmalignant and weakly malignant cells. In addition, cells with the same genotype exhibit different degrees of DNA sequestration and exposure when cytoskeletal components were selectively disrupted or when they were cultured on different ECM components.<sup>1</sup>

Without removal of oncogenes, additional deletions, or mutations, it is possible to revert cancer cells into cells that behave phenotypically normally. On two-dimensional surfaces, malignant cells can be induced by the addition of cAMP to cease blebbing, form an organized cytoskeleton, and develop contact-inhibited monolayers.<sup>2,3</sup> In a three-dimensional tissue culture system, it is possible to induce breast cancer cells to form polarized tissue structures resembling normal breast acini<sup>4,5</sup> and resume normal function,<sup>4–8</sup> including a dramatic reduction in tumor formation, and seem to function similar to differentiated breast acini. In experimental animal models, teratocarcinoma cells placed into mammalian embryos formed normal mice,<sup>9</sup> avian embryos transformed with Rous sarcoma virus<sup>10,11</sup> did not become transformed despite viral integration, and metastatic aneuploid melanoma cells placed in chick embryos<sup>12</sup> formed normal neural crest structures as they would if placed into normal adult organisms.<sup>12</sup> These findings demonstrate that the phenotypes of transformed malignant or metastatic cells are

Supported by the Department of Energy (grant DEAC03-76SF0098), the National Institutes of Health (grant EY10457), and the Norwegian Cancer Society.

Accepted for publication January 19, 2007.

Address reprint requests to Andrew J. Maniotis, Ph.D., Department of Pathology, University of Illinois at Chicago, 840 S. Wood St., 130 CSN (MC 847), Chicago, IL 60612. E-mail: amanioti@uic.edu.

highly plastic and regulated by the microenvironment into which they are placed. The mechanisms underlying these phenotypic plasticities are just beginning to be studied but are not yet understood. In addition, although there are data to indicate that changes in cell phenotype are accompanied by epigenetic changes in nuclear and chromatin organization,<sup>6,13–15</sup> little is known about global chromatin changes as a result of alternations in the microenvironment.

We used a well-characterized three-dimensional breast tumor model system<sup>4,16</sup> to determine whether the transition of tumor cells from disorganized clusters to organized, polar acinus-like structures is accompanied by global epigenetic changes in chromatin structure that could be detected by measuring changes in the resistance of DNA to specific DNA-digesting enzymes. With this technique, we show that the organization of chromatin in a malignant mammary epithelial cell line follows tissue architecture. Moreover, tissue phenotype, and DNA organization are unstable<sup>17</sup> (plastic<sup>2</sup>) and reversible. We take advantage of these observations to test the following question: is it possible to control reversibly DNA exposure and sequestration, cell polarity, tumor morphology, and, ultimately, tumor behavior through manipulation of the ECM?

## Materials and Methods

### Cell Lines and Cell Culture

MCF10A, a nonmalignant human breast epithelial cell line, was obtained from American Type Culture Collection (Rockville, MD); the spontaneously transformed and malignant human breast epithelial line HMT-3522 T4-2<sup>18</sup> was isolated by one of us (M.J.B.).<sup>6</sup> MCF10A cells were maintained in Dulbecco's modified Eagle's medium (DMEM)/F12 (BioWhittaker, Inc., Walkersville, MD) containing 20 ng/ml epidermal growth factor (Calbiochem Corp., San Diego, CA),  $1.4 \times 10^{-6}$  mol/L hydrocortisone (BD Bioscience, San Jose, CA), 0.1 ng/ml cholera toxin (Sigma, St. Louis, MO),  $10 \times 10^{-6}$  g/ml human insulin (Calbiochem Corp.), 2 mmol/L L-glutamine, 5% horse serum (Fisher, Ontario, ON, Canada), and penicillin/streptomycin. HMT-3522 T4-2 cells were routinely grown in H14 medium without 10 ng/ml epidermal growth factor on Vitrogen-coated plates (BioWhittaker, Inc.) as described previously.<sup>7</sup>

### Three-Dimensional Cultures

Three-dimensional cultures were prepared based on previously described protocols<sup>4,16</sup> with some modifications. Coverslips ( $18 \times 18$  mm) were coated with 120  $\mu$ l of reduced growth factor Matrigel (BD Bioscience). Single cell suspensions ( $0.5$  to  $1.0 \times 10^5$  cells per slip) were seeded on top of polymerized Matrigel, incubated for 30 minutes, and overlaid with 2.5 ml of culture medium containing no epidermal growth factor or serum. Cells were overlaid with medium containing 2% Matrigel. Cultures were grown for the number of days indicated in the figure legends, adding new medium every 3rd day.

### Digestion Assay

Cell smear assays were performed as described previously.<sup>1</sup> In brief, monolayer cultures grown on 10-cm dishes (70 to 90% confluent) were mechanically dislodged or trypsinized off the plate, collected by centrifugation, and resuspended in serum-free DMEM. A drop (20  $\mu$ l) of the suspension was placed on a glass slide and dried for 1 hour. DNA digestion was initiated by adding 50  $\mu$ l of serum-free DMEM containing 0.5  $\mu$ l of 10 U/ $\mu$ l *AluI* (Promega, San Luis Obispo, CA) restriction enzyme (5 U per smear) for 30 to 90 minutes and terminated by adding 1  $\mu$ g/ml ethidium bromide (Fisher Scientific) to stain DNA. Nuclei were observed and photographed with a Leica inverted fluorescent microscope (Leica, Bannockburn, IL).

DNA digestion was performed on cells in three-dimensional cultures grown for 14 days. In preliminary experiments, we first determined both the time and concentration of *AluI* required for DNA digestion, taking into account that large aggregates of T4-2 cells contain more DNA than smaller MCF10A acini. Eight hours of digestion using 60 U of *AluI* was sufficient for complete digestion of MCF10A-organized acini. The T4-2 aggregates still exhibited partial resistance to digestion after 36 hours of digestion using a total of 600 U of *AluI* (added 200 U every 12 hours), suggesting that the difference in DNA digestion is not attributable to differences in the amount of DNA contained in the three-dimensional cultures.

Both Triton X-100 (0.1%) and Nonidet P-40 (0.1%) were tested as detergents to permeabilize cells in three-dimensional cultures to explore if the detergent per se affected DNA digestion. No difference in sensitivity to DNA digestion was observed using either one of these detergents; however, when compared with cells treated with Triton X-100, the morphology of cells permeabilized with Nonidet P-40 was better restored to a round shape, making it easier to evaluate the results. Cells in three-dimensional cultures grown for 14 days were first permeabilized for 15 minutes with 0.1% Nonidet P-40, rinsed gently three times in phosphate-buffered saline (PBS), and incubated with serum-free DMEM containing *AluI* restriction enzyme (Promega) for 24 hours in an incubator at 37°C. Three-dimensional cultures of MCF10A acini, HMT-3522 T4-2 aggregates, and HMT-3522 T4-2 revertants were digested with 20  $\mu$ l of *AluI* (100 U/ml media) added twice (total 400 U/reaction) within a 24-hour incubation period. Ethidium bromide (0.5  $\mu$ g/ml) was added to label DNA at the termination of the reaction. Nuclear fluorescence was photographed with a Leica inverted fluorescent microscope. Parallel cultures in each experiment were stained with trypan blue (MP Biomedicals, Aurora, OH) to confirm complete permeabilization.

### Flow Cytometry

Cells from monolayer cultures of MCF10A and T4-2 cell lines were harvested either by scraping or trypsinization, diluted in PBS, and collected by centrifugation. The pellet was resuspended in 0.1% Nonidet P-40 and incubated for 1 minute at room temperature to permeabilize the

cells, followed by a second spin to wash away detergent. Pellets were resuspended in 0.5 ml of regular DMEM with 65 U of *AluI* and incubated for 1 hour under rotation at 37°C. Propidium iodide (1  $\mu\text{g/ml}$ ; Invitrogen/Molecular Probes, Carlsbad, CA) was added directly to each reaction at its conclusion, and the cell suspension was filtered through flow tubes with a filtered cartridge before flow cytometric analysis.

After treating T4-2 nonreverted and reverted cells from three-dimensional cultures with dispase (BD Bioscience) for 30 minutes at 37°C to degrade Matrigel proteins, cells were harvested into 15-ml Falcon tubes (BD Bioscience) and resuspended. To disperse the structures into single cell suspension, Trypsin (0.25%) was added (200  $\mu\text{l}$ ) and incubated for 5 minutes at 37°C. Single cells were collected by centrifugation and resuspended in PBS containing 1  $\mu\text{g/ml}$  propidium iodide (Invitrogen/Molecular Probes). Cell suspensions were filtered through flow tubes with a filtered cartridge and taken to flow cytometric analysis. All analyses were performed on a FACSCalibur (BD Bioscience) equipped with a 488-nm laser for forward and side scatter, and 520-, 575-, and 675-nm detectors. Each run ended at 10,000 counts and was analyzed using FACS dot-plots and histograms. Propidium iodide signal represents labeled DNA, and signal intensity of undigested DNA (approximately corresponding to fluorescent intensity  $10^2$  to  $10^4$ ) was gated as M2. Lower signal intensity representing digested DNA (shorter DNA fragments) was gated as M1.

### *Phenotypic Tumor Reversion with PI3K Inhibitor and or Dibutyl-cAMP*

Cells were seeded on Matrigel as described above, overlaid with 2.5 ml of growth medium containing 8  $\mu\text{mol/L}$  PI3K inhibitor LY294002 (Calbiochem/EMD Biosciences, Inc., San Diego, CA) or a combination of 6  $\mu\text{mol/L}$  LY294002 and 1 mmol/L *N*<sup>6</sup>-dibutyl-cAMP (Sigma-Aldrich, St. Louis, MO). Cultures were maintained for 14 days with addition of new drugs every 3rd day. No toxicity was observed in either normal or tumorigenic three-dimensional cultures of mammary epithelial cells at these drug concentrations. Dibutyl-cAMP analog, in addition to elevating cAMP within the cell, metabolizes to butyrate, which alone is known to have distinct biological effects. However, sodium butyrate, in concentrations ranging from 1 to 2 mmol/L, did not induce tumor reversion when added to the T4-2 cell cultures, thus eliminating a possible butyrate effect involved in tumor reversion. In experiments testing cAMP analog specificity and tumor reversion, cells were seeded as above and overlaid with medium containing either 0.5 mmol/L 8-CPT-2'-*O*-Me-cAMP (BioLog Life Science, Bremen, Germany) or 0.5 mmol/L *N*<sup>6</sup>-monobutyl-cAMP (BioLog Life Science).

### *Phenotypic Tumor Reversion with Antibodies to ECM Proteins*

Cells were seeded on Matrigel as described above and overlaid with 2.5 ml of medium containing one of the

following antibodies: rabbit anti-human fibronectin (FN) (A0245, 1:100 dilution; DAKO, Carpinteria, CA), mouse anti-human laminin (Lam-89, 1:100 dilution; Sigma-Aldrich), mouse anti-human collagen IV (CIV22, 1:100 dilution; DAKO), rabbit anti-human collagen I (CL50111AP, 1:100 dilution; Cedarlane, Hornby, ON, Canada), and mouse anti-human  $\gamma$ -tubulin (Sigma-Aldrich). The cultures were fed every 3rd day by overlay with 1 ml of medium containing fresh antibody. Because the antibody solvent contains low concentrations of sodium azide, we tested for any effects that sodium azide might have on tumor reversion in a separate series of experiments and discovered that sodium azide had no effect by itself or in combination with control antibodies used in these experiments (data not shown).

### *Immunofluorescence Microscopy*

Cells were cultured on top of a Matrigel-covered coverslip for 14 days as described above. Coverslips were washed three times with cytoskeleton extraction buffer (50 mmol/L HEPES, 300 mmol/L sucrose, 100 mmol/L KCl, 5 mmol/L MgCl<sub>2</sub>, 5 mmol/L ethylenediaminetetraacetic acid, and 0.5% Triton X-100) containing 1 mmol/L sodium orthovanadate, 20 mmol/L sodium fluoride, and 20  $\mu\text{l/ml}$  protease inhibitor cocktail from Sigma-Aldrich for 3 seconds, rinsed with 1 $\times$  PBS, and fixed in 100% ice-cold methanol (5 minutes at  $-20^\circ\text{C}$ ) followed by 5 minutes of incubation in ice-cold 100% acetone. Cells were rinsed three times in 1 $\times$  PBS and incubated overnight at 4°C with mouse anti-human  $\beta_4$  integrin (clone E31) at a 1:200 dilution (Chemicon, Temecula, CA) or mouse anti- $\beta$ -catenin (clone 14) at 5  $\mu\text{g/ml}$  dilution (BD Transduction Laboratories, San Jose, CA). Slides were washed three times for 2 to 5 minutes, incubated with a 1:200 dilution of goat anti-mouse secondary antibody conjugated to Alexa Fluor 546 (Molecular Probes) for 30 minutes, washed three times (as above), and mounted on glass slides in Vectashield mounting medium (Vector Laboratories, Burlingame, CA). Control cultures for all experiments were treated with the same concentration of nonspecific rabbit IgG (catalog no. ab27478; Abcam, Cambridge, MA). The cultures were fed every 3rd day by overlay of 1 ml of medium containing fresh antibody.

### *Laser-Scanning Confocal Microscopy*

Confocal images were taken on a Zeiss LSM510 laser-scanning microscope (Carl Zeiss Micro Imaging Inc., Thornwood, NY) using incident light fluorescence and differential interference contrast (DIC) with  $\times 25$  and  $\times 63$  water immersion objectives. An argon laser was applied for red fluorescence (Alexa Fluor 546 and EtBr<sub>2</sub> at 543-nm wavelength) and a UV laser for blue fluorescence (4,6-diamidino-2-phenylindole at 405-nm wavelength). Images were captured using LSM Software Release 2.5 (Carl Zeiss, Thornwood, NY) on a standard high-end Pentium PC (Fujitsu-Siemens, Maarssen, The Netherlands).

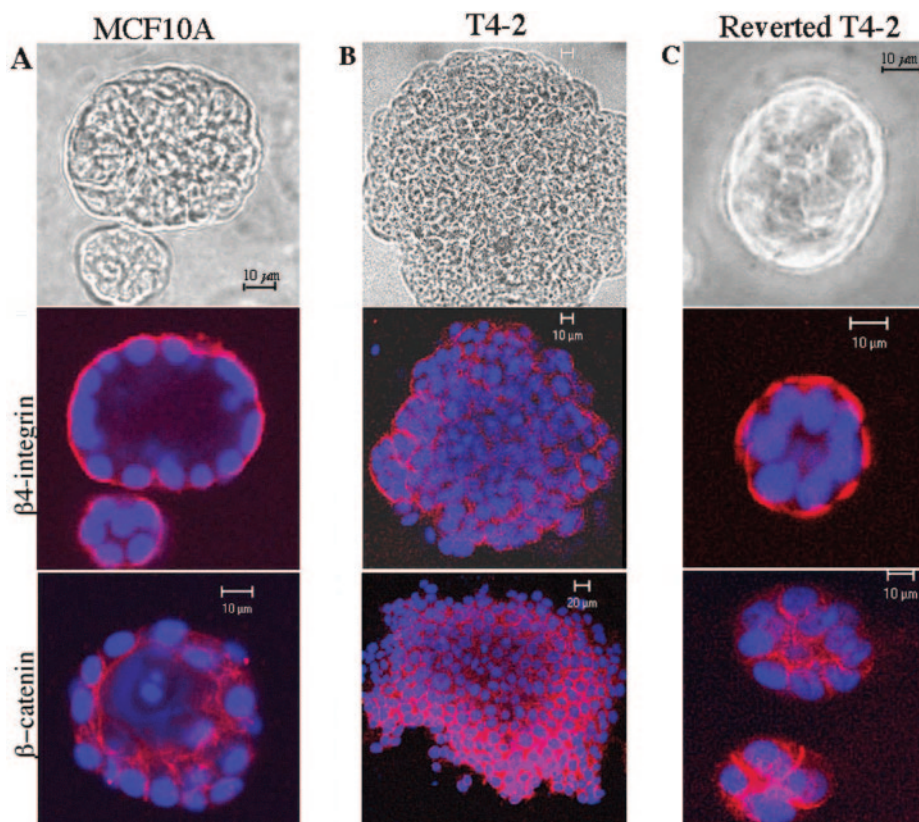


**Figure 1.** Restoration of mammary cell polarization and morphogenesis from tumorigenic to normal by the combination of LY294002 PI3K inhibitor and dibutyryl-cAMP. Compare the architecture and distribution of  $\beta 4$ -integrin and  $\beta$ -catenin between MCF10A breast epithelial cells (A) and transformed T4-2 tumorigenic breast cells (B), and T4-2 cells that were reverted after exposure to the combination of LY294002 PI3K inhibitor and dibutyryl-cAMP (C). Reverted T4-2 cells resemble MCF10A cells in the size and architecture of the aggregates, and the distribution of  $\beta 4$ -integrin and  $\beta$ -catenin are identical. By contrast, aggregates formed by transformed T4-2 cells are large and disorganized, and the distribution of  $\beta 4$ -integrin and  $\beta$ -catenin is haphazard. On the top row, MCF10A cells (A) and T4-2 cells (B) are illustrated with DIC microscopy, and reverted T4-2 cells are illustrated by phase microscopy (C).

## Results

### Phenotypic Reversion of Tumorigenic T4-2 Cells

The behavior of T4-2 tumorigenic cells in three-dimensional culture conditions was compared with MCF10A breast epithelial cells. After 10 to 14 days, MCF10A cells formed polarized acini with the nuclei arranged circumferentially around the hollow interior.<sup>16</sup>  $\beta 4$ -Integrin was distributed in a circular ring, facing the ECM environment, and  $\beta$ -catenin was identified internally on cell surfaces between different cells comprising the multicellular acini (Figure 1A). By contrast, within a few days, T4-2 cells developed into disorganized aggregates that were considerably larger than polarized structures formed by MCF10A cells (note differences in scale bar sizes, Figure 1). In the disorganized T4-2 aggregates,  $\beta 4$ -integrin distribution was observed on cell surfaces facing all directions, both between cells and on surfaces facing the extracellular environment. In addition, in the disorganized T4-2 aggregates,  $\beta$ -catenin was distributed in and between most of the cells (Figure 1B). Compared with the architecture of MCF10A acini, the disorganized T4-2 aggregates seemed to have completely lost polarization.

Tumorigenic T4-2 cells can be induced to develop into architecturally normal acinus-like structures in three-

dimensional cultures when treated with a PI3K inhibitor.<sup>8,17</sup> We confirmed these results for reversion of tumorigenic T4-2 cells by culturing on Matrigel in the presence of 8  $\mu\text{mol/L}$  PI3K inhibitor LY294002 (not shown).<sup>4,7,8,17</sup> We also obtained phenotypic reversion using dibutyryl-cAMP at a concentration of 1 mmol/L (not shown), consistent with previous observations of phenotypic tumor reversion in monolayer cultures.<sup>2</sup>

A combination of 6  $\mu\text{mol/L}$  LY294002 PI3K inhibitor and 1 mmol/L dibutyryl-cAMP induced the formation of reverted structures most similar to the acini formed by MCF10A cells in terms of size, polarity, and lumen formation (Figure 1C). In the acini-like structures formed by the reverted T4-2 cells, a dense ring of  $\beta 4$ -integrin surrounded each spheroid, similar to the ring of integrin formed around MCF10A acini. In addition,  $\beta$ -catenin was redistributed from a disorganized haphazard pattern in the nondrug-treated T4-2 aggregates to a lace-like or stellar pattern of the drug-treated structures that closely resembled  $\beta$ -catenin distribution in MCF10A cells in three-dimensional culture conditions (Figure 1, compare B and C). Moreover, acinus-like structures formed by T4-2 cells exposed to the combination of LY294002 PI3K inhibitor and dibutyryl-cAMP were hollow, similar to the MCF10A acini. Therefore, because of the degree of fidelity we observed in the architecture of the revertants com-

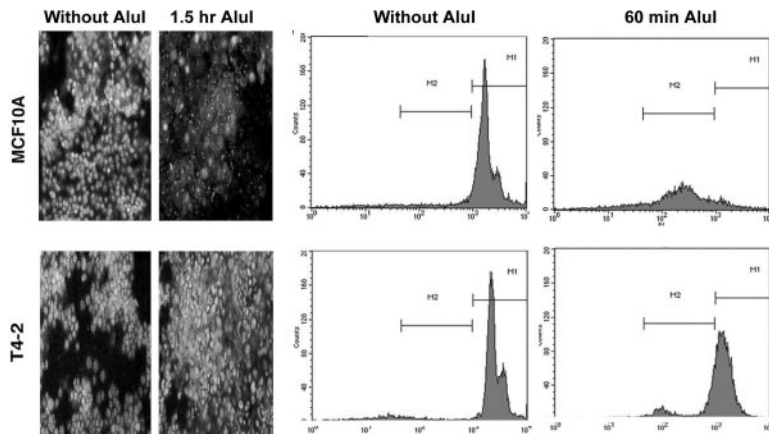


**Figure 2.** Differential DNA digestion of MCF10A and T4-2 cells in two-dimensional cultures by *AluI* restriction enzyme. The digestion of chromatin before and after 1.5 hours of exposure to *AluI* was compared between MCF10A and T4-2 tumorigenic cells after the cells were smeared as monolayers and dried onto slides. Chromatin was visualized by fluorescence microscopy after staining with ethidium bromide. Differential digestion of chromatin in T4-2 tumorigenic cells was also demonstrated by flow cytometry after 60 minutes of digestion by *AluI*. Percent DNA digestion is determined by relative increase of fluorescent intensity gated in M1 before and after digestion. The results illustrated are representative of five repeats of each experiment and are consistent with previous observations that in two-dimensional conditions, the chromatin of malignant cells of various histological origins is more sequestered to *AluI* than the chromatin of nonmalignant cells.<sup>1</sup>

pared with normal MCF10A structures when using the combination of 6  $\mu\text{mol/L}$  LY294002 PI3K inhibitor and 1  $\text{mmol/L}$  dibutyryl-cAMP, this treatment was used as our standard protocol to consistently induce revertants exhibiting acinus-like structures with size and phenotype most similar to MCF10A acini.

### Differential DNA Digestion in Nonmalignant versus Tumorigenic Mammary Epithelial Cells Grown in Two-Dimensional Cultures

In the cell-smear assay we developed previously,<sup>1</sup> the DNA of MCF10A cells was extensively digested after a 1.5-hour exposure to *AluI* restriction enzyme. By contrast, DNA in the nuclei of T4-2 cells appeared to be mostly undigested after 1.5 hours of exposure to *AluI*. To confirm these qualitative observations, DNA digestion was quantified by flow cytometry. Under these conditions, a shift in the DNA profile of MCF10A cells was dramatically more than that observed for T4-2 cells after 60 minutes of *AluI* digestion (Figure 2).

### Differential DNA Digestion in Normal versus Tumorigenic Mammary Epithelial Cells Grown in Three-Dimensional Cell Cultures

To explore the sensitivity of DNA to *AluI* restriction enzyme of cells exhibiting three-dimensional architectural structure we developed an assay for the digestion of cells in three-dimensional culture conditions by *AluI* (see Materials and Methods). MCF10A epithelial cells and T4-2 tumorigenic breast carcinoma cells were cultured for 14 days on Matrigel and allowed to form growth-arrested acini or large disorganized aggregates, respectively (see Figure 1). After permeabilization with 0.1% Nonidet P-40 for 10 minutes, the nuclei and cell morphology remained intact in the three-dimensional cultures of MCF10A and transformed T4-2 cells, respectively (Figure 3A). Furthermore, these conditions allowed sufficient permeabilization for complete uptake of trypan blue in small acini or acinus-like structures of MCF10A, reverted T4-2, and large transformed T4-2 aggregates (Figure 3B), indicat-

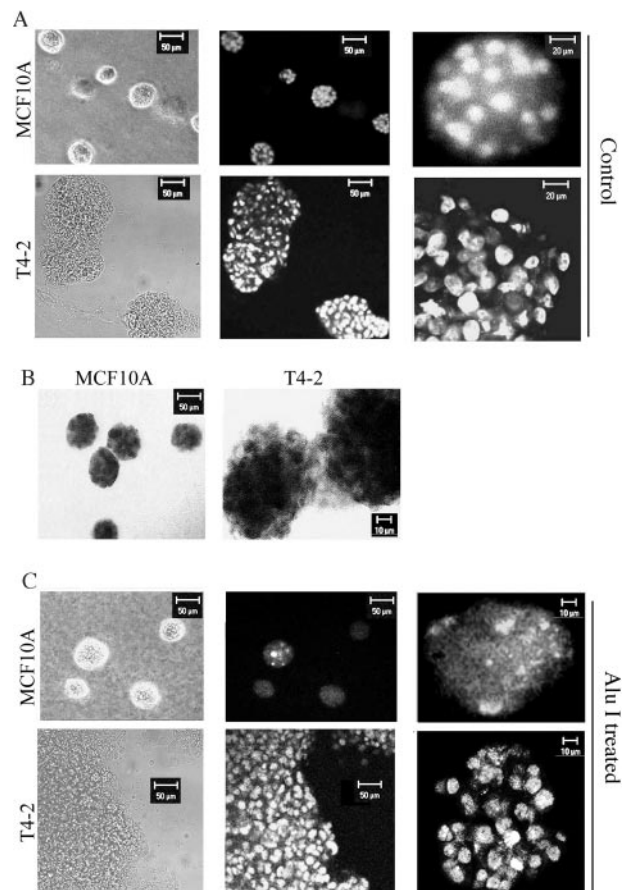


**Figure 3.** Differential DNA digestion in normal versus tumorigenic mammary epithelial cells grown in three-dimensional cell cultures. MCF10A cells formed small aggregates after 2 weeks on Matrigel, and T4-2 tumorigenic breast cells formed larger, disorganized aggregates under the same conditions. **A:** The nuclei within both MCF10A and T4-2 cells stained brightly with ethidium bromide. **B:** After permeabilization of MCF10A and T4-2 aggregates with 0.1% Nonidet P-40 for 10 minutes, these aggregates stained with trypan blue, indicating complete permeabilization (T4-2 cells reverted to form acini also incorporated trypan blue, not shown). After permeabilization as described above followed by exposure to *AluI* for 24 hours and staining with ethidium bromide, the chromatin in cells forming MCF10A aggregates digested, whereas the chromatin in T4-2 cells resisted digestion. **C:** Thus, the differential sensitivity of benign MCF10A cells to *AluI* compared with T4-2 tumorigenic cells seen in two-dimensional conditions (Figure 2) is extended to three-dimensional conditions.

ing that the three-dimensional structures were completely permeabilized.

After incubation with *AluI* for 24 hours, the chromatin in MCF10A acini was completely digested, and by contrast, chromatin in T4-2 cells forming disorganized aggregates resisted digestion in the same time period under identical conditions (Figure 3C). Thus, the chromatin of MCF10A cells assembled into acini was far more sensitive to *AluI* digestion than the chromatin of T4-2 cells assembled into disorganized multicellular aggregates.

### Reversible Manipulation of Phenotype and DNA Sequestration

We applied the reversible T4-2 system to test whether there is a differential sensitivity to *AluI* of the DNA in reverted T4-2 cells forming acinus-like structures, compared with DNA in transformed T4-2 cells forming disorganized aggregates. We observed that the DNA in T4-2 disorganized aggregates (Figure 3C) was far more resistant to digestion than the DNA in T4-2 cells induced to form acinus-like structures (revertants), by either PI3K inhibitor (not shown) or the PI3K inhibitor plus dibutyryl-cAMP (Figure 4A), indicating that phenotypic tumor reversion is accompanied by a significant shift in chromatin sequestration.

Exposure of T4-2 cells to PI3K inhibitor plus dibutyryl-cAMP (Figure 4B) resulted in the formation of organized acinus-like structures composed of cells containing chromatin that digested completely with *AluI* restriction enzyme. When the PI3K inhibitor and dibutyryl-cAMP were removed throughout a 14-day period, the reverted T4-2 acinus-like structures began to enlarge, became disorganized, and were phenotypically identical to control, nonreverted T4-2 cell aggregates (Figure 1B). As the reverted T4-2 cells changed morphologically from organized spheroids (day 0) to disorganized spheroids (day 7) and to disorganized aggregates without any evidence of polarity (day 15), DNA became more resistant to digestion with *AluI* restriction enzyme (Figure 4B). Quantification using flow cytometry confirmed the visual comparisons of DNA digestion experiments (Figure 4). Taken together, reversible manipulation of three-dimensional cultures from a tumor-like architecture to a normal architecture and back again was consistently accompanied by reversible changes in DNA sequestration.

### Manipulation of Morphology, Polarization, and Chromatin Sensitivity to DNA Digestion Specifically Involves a Protein Kinase A (PKA)-Coupled Signal

Dibutyryl-cAMP has been reported to induce reverse transformation of a number of transformed cell lines grown in monolayer.<sup>2</sup> Treatment with 1 mmol/L dibutyryl-cAMP was reported in 12 different tumorigenic cell lines to restore normal morphology and sensitivity to nuclear chromatin digestion by DNase I. Cyclic AMP has traditionally been thought to act exclusively through the

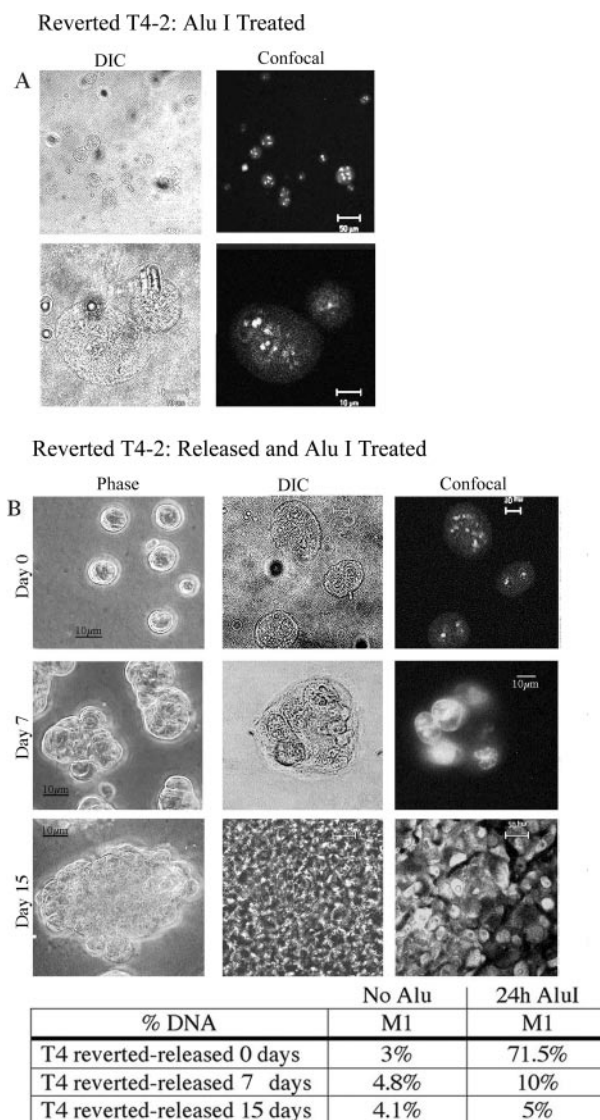


**Figure 4.** Reversible manipulation of phenotype and genome sequestration. As shown in Figure 1C, T4-2 cells grown for 2 weeks on Matrigel can be reverted to form polarized acini with 6  $\mu\text{mol/L}$  LY294002 and 1 mmol/L dibutyryl-cAMP. DNA digested when these revertants were permeabilized and exposed to *AluI* for 24 hours followed by labeling with ethidium bromide (**A**, matched laser-scanning confocal microscopy and DIC for two magnifications). Note in the higher magnification images (**A**, bottom row) that only the nucleoli remain undigested in the nuclei of completely digested T4-2 revertants. These data are representative images of observations obtained from five separate identical experiments. Compare with Figure 3C illustrating the resistance of chromatin in nonreverted T4-2 cells grown under identical conditions. To determine whether chromatin exposure in T4-2 cells that have been reverted to polarized acini is reversible, these acini were gradually released from exposure to 6  $\mu\text{mol/L}$  LY294002 and 1 mmol/L dibutyryl-cAMP at day 0, and the preparations were subjected to digestion by *AluI* for 24 hours followed by staining with ethidium bromide (**B**). Note that changes in morphology from an acinus (day 0) to a large disorganized aggregate (day 15) as visualized by DIC and phase microscopy is accompanied by increased sequestration of chromatin. These data are representative for three separate identical experiments. The percentage of digested DNA before and after *AluI* digestion on revertant T4-2 at day 0, day 7, and day 15 after drug release (similar to above) by flow cytometry summarized for three experiments is summarized in the table.

cAMP-dependent PKA,<sup>19,20</sup> and effects of cAMP on tumor reversion have been attributed to activation of PKA.<sup>21,22</sup> However, the action of intracellular cAMP is not only mediated by PKA but also by a newly recognized

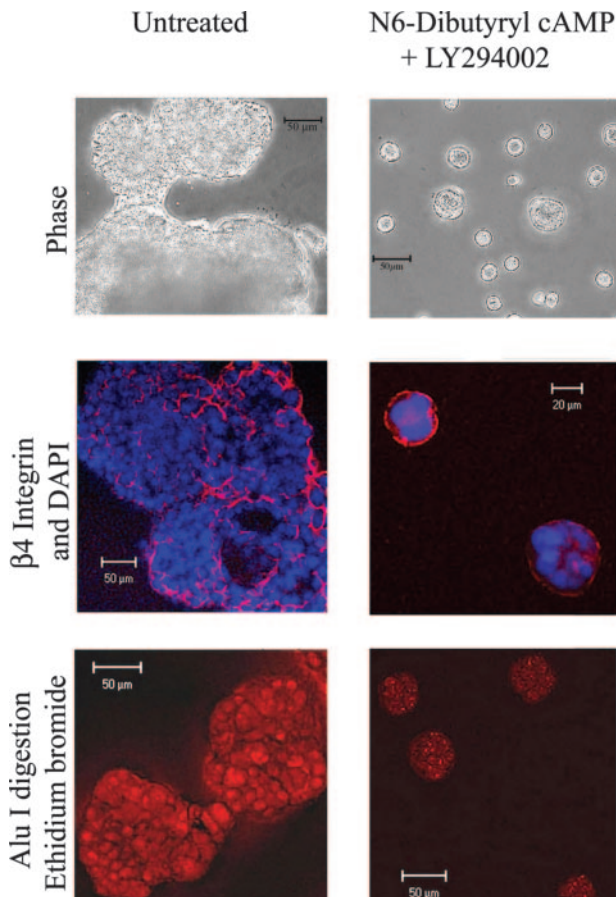


**Figure 5.** cAMP-induced reversion of morphology, polarization, and chromatin organization involves a PKA-coupled signal. Note that after treatment with *N*<sup>6</sup>-monobutyryl-cAMP, disorganized large T4-2 aggregates reorganize into small polarized acinus-like structures as reflected by the distribution of  $\beta 4$ -integrin (compare with Figure 1). Reversion to the acinus-like morphology is accompanied by sensitivity of *AluI* restriction enzyme. These data are representative for three separate identical experiments.

family of cAMP-binding proteins designated as cAMP-regulated guanine nucleotide exchange factors (also known as *Epac*).<sup>23,24</sup>

To discriminate between *Epac*- and PKA-coupled signals, we tested specific cAMP analogs for their ability to revert T4-2 cells in three-dimensional cultures. Monobutyryl-cAMP, which is a poor agonist for *Epac* but a potent PKA activator,<sup>25,26</sup> phenotypically reverted the T4-2 cells into organized acinus-like struc-

tures (Figure 5), as was seen for T4-2 cells treated with PI3K inhibitor plus dibutyryl-cAMP (Figure 2).  $\beta 4$ -Integrin distribution within the monobutyryl-cAMP-reverted acinus-like structures appeared on the cell basal surfaces facing the microenvironment, and these reverted structures appeared to be hollow in the center, indicating both basal and apical polarization (Figure 5). Furthermore, the nuclei of these reverted T4-2 spheroids were also sensitive to DNA digestion by *AluI* (Figure 5). Parenthetically, the 8-CPT-2P-O-Me-cAMP analog (a selective and strong agonist for *Epac*<sup>24</sup>) did not revert tumorigenic T4-2 cells into polarized acinus-like structures:  $\beta 4$ -integrin was randomly distributed on cell surfaces throughout the disorganized cell aggregates, and the nuclei were resistant to DNA digestion by *AluI* similar to untreated T4-2 cells (Figure 5).

#### *Antibody Interference of FN Drives Phenotypic Tumor Reversion, Induces Polarization, and Exposes Sequestered DNA*

To determine whether changes in the interaction between T4-2 cells (forming either aggregates or reverted acinus-like structures) and the ECM influenced the phenotype, structural polarity, and DNA organization, T4-2 cells were cultured in Matrigel with antibodies targeting individual human ECM components including FN, collagen I (Col I), collagen IV (Col IV), and laminin (LM) (Table 1 and Figure 6).

T4-2 cells exposed to anti-Col I antibody or anti-Col IV antibody assembled into spherical aggregates whereas T4-2 cells treated with anti-LM assembled into horizontal plaque-like structures (Figure 6A). However, as early as 6 to 7 days (data not shown) and more pronounced by day 14 when compared with cultures treated with IgG as a control, anti-FN antibody treatment reverted the T4-2 cells to acinus-like morphology, indistinguishable from revertants produced via the combination of PI3K inhibitor and dibutyryl-cAMP or with monobutyryl-cAMP analog alone (compare Figure 6A with Figure 5).

Moreover, the T4-2 cultures exposed to anti-FN antibody assembled into polar acini with hollow lumens and  $\beta 4$ -integrin on the basal surface, morphological traits identical to those observed by T4-2 cells when stimulated to revert by cAMP cocktail (Figure 6B). By contrast, anti-

**Table 1.** The Effects of Treatment on Morphology and the Sequestration or Exposure of DNA

T4-2 cultures*	Morphology	Polarization†	DNA digestion‡
Untreated	Disorganized aggregate	–	Resistant
LY249002/dibutyryl-cAMP	Acinus-like	+	Sensitive
Anti-fibronectin	Acinus-like	+	Sensitive
Anti-collagen I	Spheroid	–	ND
Anti-collagen IV	Spheroid	ND	ND
Anti-laminin	Horizontal plaque	–	Resistant
Control IgG	Disorganized aggregate	–	Resistant

ND, not determined.

\*Cultures of T4- cells grown in three dimensions for 14 days in the presence of different agents (as indicated) before being analyzed.

†Determined by  $\beta 4$ -integrin distribution (revealed by immune staining) and hollow lumen (revealed by nucleus orientation). See Materials and Methods.

‡The sensitivity of DNA was determined by 24-hour *AluI* digestion (see Materials and Methods).

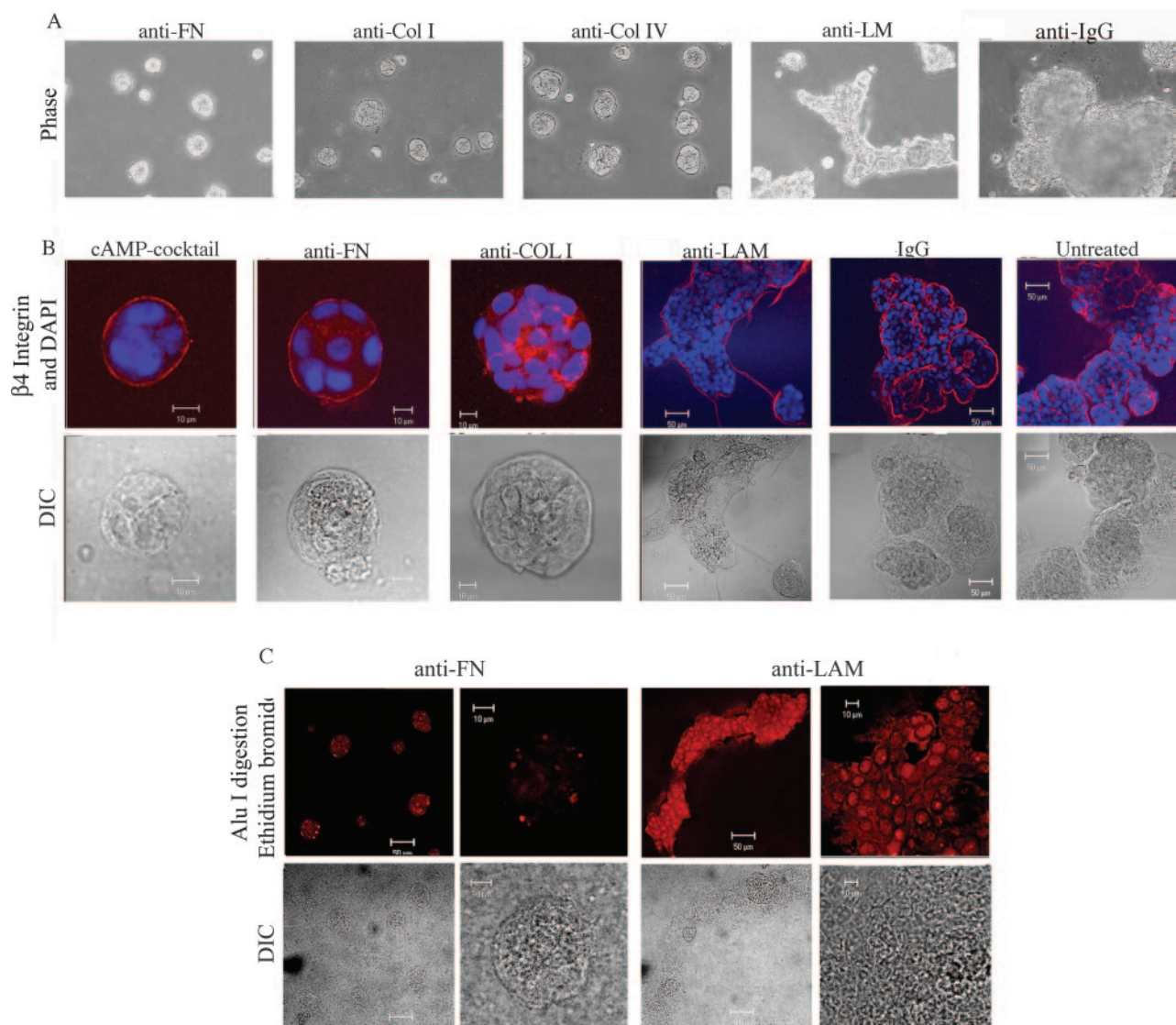


**Figure 6.** Reversion of morphology, polarization, and chromatin organization by interfering with the communication of ECM components. **A:** Phase micrographs comparing the morphology of T4-2 cells grown for 14 days on Matrigel in the presence of different antibodies: anti-FN, anti-collagen I (anti-COL I), anti-collagen IV (anti-COL IV), anti-laminin (anti-LAM), and nonspecific IgG. **B:** Anti-FN induced reversion of T4-2 cells to acini featuring a distribution of  $\beta 4$ -integrin identical to that seen after these cells are reverted to polarized acini with the cAMP cocktail and identical in morphology and distribution of  $\beta 4$ -integrin in MCF10A cells (compare with Figure 1). Anti-collagen I induced T4-2 cells to form small aggregates, but the distribution of  $\beta 4$ -integrin is haphazard and not confined to the acinar surface. Neither anti-laminin nor control IgG altered the organization of T4-2 aggregates or the distribution of  $\beta 4$ -integrin. **C:** The association between morphology and sensitivity of *AluI* restriction enzyme. The chromatin of disorganized T4-2 aggregates resists digestion by *AluI*, but chromatin from the same cells that had reverted to acinar morphology after cAMP cocktail was sensitive to *AluI*. The chromatin of T4-2 cells reverted by anti-FN was susceptible to digestion by *AluI* (illustrated at two magnifications), but the chromatin in disorganized T4-2 aggregates treated with anti-laminin resisted digestion with *AluI* (also shown at two magnifications) similar to the behavior of untreated T4-2 cells. Original magnifications,  $\times 200$  (A).

Col I antibody induced spherical structures, but they did not appear hollow nor were they polarized as suggested by the random distribution of  $\beta 4$ -integrin. Anti-LM antibody-treated cultures also did not appear to be polarized and exhibited long strings of  $\beta 4$ -integrin staining between the horizontal cell plaques. Cells grown in the presence of nonspecific IgG served as a negative control with respect to polarization and behaved similar to untreated cultures (Figure 6B). Remarkably, DNA in anti-FN-treated polarized revertants completely digested after 24-hour exposure to *AluI*. The cells in the plaque-like anti-LM-treated cultures, by contrast, harbored chromatin that was resistant to 24 hours of *AluI* digestion, similar to

chromatin in the transformed T4-2 aggregates (Figure 6C). Thus, there is a strong association between reversion of morphology and chromatin sequestration as measured by sensitivity to *AluI* restriction enzyme.

To address the possibility that the inhibitors act on chromatin structure when T4-2 cells are grown in two-dimensional culture conditions, T4-2 cells were grown as flat monolayers and treated with cAMP, the cAMP cocktail, or anti-FN. Such treatments produced no significant change in the organization of the monolayer. Furthermore, the exposure of untreated T4-2 cells or cells treated with these reagents to increasing concentrations of these reversion agents did not produce a significant

difference in cell morphology or in DNA digestion regardless of whether the cells were cultured on plastic or collagen (data not shown).

## Discussion

We have shown that the DNA of nonmalignant breast epithelial cells that form polarized acini, are exposed to *AluI* digestion, whereas tumorigenic cells that form disorganized, nonpolarized aggregates, exhibit profound sequestration of their DNA under identical enzymatic digestion conditions. Tumorigenic T4-2 cells induced to form polarized acinus-like structures displayed a level of sensitivity to *AluI* that was comparable with that observed in MCF10A cells when assembled into acini. Thus, the process of T4-2 cell polarization and assembly into an acinus-like structure shifted the chromatin organization of these cells, causing previously sequestered DNA to assume a more open conformation with increased accessibility to *AluI*. In addition, when established reverted T4-2 acinus-like structures are released from agents that induce polarity, they grow into disorganized, unpolarized aggregates. This shift from a reverted to a tumorigenic morphology is accompanied by a shift in chromatin organization from an exposed to a sequestered state. From these results, we conclude that chromatin organization is coupled to tissue architecture and can be reversibly manipulated. More specifically, chromatin organization is linked to tissue polarity and the three-dimensional organization of cells in an extracellular environment.

Many different *in vitro* and *in vivo* observations support the fact that transformations in phenotype and DNA sequestration are not enzymatic artifacts.<sup>1</sup> For instance, we previously showed that the DNA in human cancer cells is tightly packaged *in vitro*, making it less susceptible to digestion by restriction enzymes.<sup>1</sup> Most importantly, touch preparations made to compare human lesions with their margins in the normal tissue all demonstrate that the more invasive the cancer, the more its DNA is protected from restriction enzyme cleavage.<sup>1</sup> Therefore, enhanced DNA protection has now been observed in many different types of cancer and is reversible, suggesting that DNA rearrangements as described here may be a universal feature of malignant cells. Sequestration of DNA may serve as a physical marker for malignancy in breast cancer and may be applicable in other types of cancer detection as well. Therefore, chromatin organization analysis may be a supplement for current methods of cancer diagnostics that detect chemical markers that are highly variable from tumor to tumor and from patient to patient or that are highly specific for certain types of tumors.

In devising the most optimal conditions for generating polarized acinus-like structures from T4-2 cells, we discovered that a cocktail of two reagents, which alone can revert T4-2 cells, produced the most consistent development of acinus-like, polarized structures. These reverted structures resembled the polarized acini generated by nonmalignant MCF10A cells. This finding supports previous studies using PI3K inhibitor<sup>3</sup> or an analog of dibutyryl-cAMP for tumor reversion.<sup>3,22</sup> In addition, we show

for the first time that cAMP can revert cancer cells in a three-dimensional context. Biochemically, the action of intracellular cAMP can be attributed to activation of at least two intracellular substrates: PKA and EPAC.<sup>23,24</sup> Using specific cAMP-analogs that discriminate between the activation of these substrates,<sup>25,26</sup> we found that the reversion of T4-2 morphology, polarity, and *AluI* sensitivity involves a PKA-coupled signal.

Unraveling the complexity of DNA packaging or sequestration in its native state within the intact cell nucleus may suggest a new possible mechanistic explanation of how eukaryotic genes are turned on or off and how they are reversibly expressed or suppressed. From a mechanistic point of view, these experiments using *in situ* DNA digestion with *AluI* indicate that higher order structure of native chromatin is organized such that the sequestration and exposure of DNA is linked to cytoarchitecture (cell polarity, cell shape, acinus three-dimensional architecture). Because DNA, as the substrate, must be exposed to *AluI* (the enzyme) to be digested, the reversible changes we observed in *AluI* sensitivity suggests that proteins organizing higher order chromatin structure are capable of reversibly enveloping the DNA as a tightly wrapped spring. Such a hypothesis provides a mechanistic picture of how chromatin fibers in a higher order conformation in living cells dynamically interact with one another to expose or sequester specific DNA sequences in regular patterns. This may in turn account for specific malignant cancer, nonmalignant cancer, or normal gene expression and phenotypic expression types.

When tumorigenic viruses, or highly invasive tumor cells, are placed into embryos, tumors do not form, suggesting that the behavior of cancer is contextual.<sup>9,10,12</sup> These studies demonstrate that when highly invasive tumor cells are placed into the complex milieu of soluble and insoluble factors within the embryo, they become regulated, to behave as normal cells, without causing cancer in the mosaic organism that develops. If tumor cells are implanted early enough during embryogenesis, some of the tumor cells are passed down through the germ line and to the mosaic organism's descendants without causing cancer in these mosaic organisms.<sup>9</sup> Importantly, context-regulation of cancer cells in the embryonic environment occurs even when the cancer cells have already metastasized from their primary tumor site.<sup>12</sup> This suggests that context regulation of cancer cells is possible despite deregulation of proteins, cell structure, cell cycle, or telomerase activity and occurs independent of mutations, aberrations of oncogenes, and aneuploidy.

It is known that the ECM by itself can provide signals that are relayed from integrin receptors on the cell surface to the nucleus by the cytoskeleton.<sup>27-29</sup> Therefore, we explored if tumor reversion, and the accompanying chromatin reorganization, could be obtained by interfering only with specific cues from the ECM using antibodies to proteins found in our malignant tumor samples. In particular, we specifically targeted those ECM components that have been reported to be highly expressed by various tumors.<sup>30-32</sup> The different antibodies used all induced profound changes in the development and the

resulting morphology of T4-2 structures (see Table 1 and Figure 5). Of key importance, the structures induced by treatment with an anti-FN antibody exhibited chromatin that was exposed in an identical manner to chromatin of normal acini and chromatin in acinus-like structures produced by cAMP and PI3K inhibitor. By contrast, and at the other extreme, the anti-laminin antibody induced structures that exhibited chromatin that was sequestered.

By placing T4-2 cells in the context of a laminin-rich matrix in the presence of a single component such as anti-FN, complete phenotypic reversion from normal to tumorigenic phenotype is observed, and DNA becomes exposed from the sequestered state. Furthermore, changes in both phenotype and DNA exposure are reversible. These observations suggest that the components of the tumor microenvironment can be identified, isolated, and perhaps therapeutically exploited, as indicated in the reversion obtained with a single molecular species such as anti-FN.

Specific isoforms of FN that are normally expressed in fetal tissue<sup>33,34</sup> but rarely expressed in adult tissue, have been detected in different cases of human cancer.<sup>35</sup> In addition, the B-isoform of FN (EDB-FN) plays a role in cellular transformation and tumor pathogenesis,<sup>36-41</sup> and a truncated isoform of FN referred to as fetal migration stimulatory factor has been detected in the serum of 90% of breast cancer cases,<sup>42</sup> as well as in other human cancers.<sup>36,43,44</sup> Elucidating the mechanisms through which ECM components influence tumor cell and DNA organization may lead to the identification of new potential targets for cancer therapy.

In summary, 1) information conveyed from the ECM environment controls tissue phenotype, cellular and organoid, polarity, and DNA sequestration or exposure; 2) shifts in cellular polarity and chromatin organization are concomitant events; and 3) agents targeting multiple signaling pathways (eg, PI3K, PKA, and FN) evoke identical phenotypes in cell morphology and chromatin organization. The causal determinants of indolent or malignant cancer cell behavior and chromatin organization seem to be epigenetic rather than genetic in nature, and these signaling pathways can be manipulated from outside of tumor cells by selecting specific molecular targets within the ECM.

## Acknowledgments

We thank Dr. M. Chen at the Research Resource Center (University of Illinois at Chicago) for expert assistance with confocal and helpful discussions and Professor Stein Ove Doseland at the Department of Biomedicine (University of Bergen, Bergen, Norway) for providing cAMP analogs and for helpful advice and discussions. We dedicate this work in memory of Dr. Theodore Puck.

## References

1. Maniotis AJ, Valyi-Nagy K, Karavitis J, Moses J, Boddipali V, Wang Y, Nunez R, Setty S, Arbieva Z, Bissell MJ, Folberg R: Chromatin organization measured by AluI restriction enzyme changes with malignancy and is regulated by the extracellular matrix and the cytoskeleton. *Am J Pathol* 2005, 166:1187-1203

2. Krystosek A, Puck TT: The spatial distribution of exposed nuclear DNA in normal, cancer, and reverse-transformed cells. *Proc Natl Acad Sci USA* 1990, 87:6560-6564
3. Puck TT, Webb P, Johnson R: Cyclic AMP and the reverse transformation reaction. *Ann NY Acad Sci* 2002, 968:122-138
4. Weaver VM, Petersen OW, Wang F, Larabell CA, Briand P, Damsky C, Bissell MJ: Reversion of the malignant phenotype of human breast cells in three-dimensional culture and in vivo by integrin blocking antibodies. *J Cell Biol* 1997, 137:231-245
5. Wang F, Weaver VM, Petersen OW, Larabell CA, Dedhar S, Briand P, Lupu R, Bissell MJ: Reciprocal interactions between beta1-integrin and epidermal growth factor receptor in three-dimensional basement membrane breast cultures: a different perspective in epithelial biology. *Proc Natl Acad Sci USA* 1998, 95:14821-14826
6. Lelievre SA, Weaver VM, Nickerson JA, Larabell CA, Bhaumik A, Petersen OW, Bissell MJ: Tissue phenotype depends on reciprocal interactions between the extracellular matrix and the structural organization of the nucleus. *Proc Natl Acad Sci USA* 1998, 95:14711-14716
7. Weaver VM, Lelievre S, Lakins JN, Chrenek MA, Jones JC, Giancotti F, Werb Z, Bissell MJ: Beta4 integrin-dependent formation of polarized three-dimensional architecture confers resistance to apoptosis in normal and malignant mammary epithelium. *Cancer Cell* 2002, 2:205-216
8. Wang F, Hansen RK, Radisky D, Yoneda T, Barcellos-Hoff MH, Petersen OW, Turley EA, Bissell MJ: Phenotypic reversion or death of cancer cells by altering signaling pathways in three-dimensional contexts. *J Natl Cancer Inst* 2002, 94:1494-1503
9. Mintz B, Illmensee K: Normal genetically mosaic mice produced from malignant teratocarcinoma cells. *Proc Natl Acad Sci USA* 1975, 72:3585-3589
10. Dolberg DS, Bissell MJ: Inability of Rous sarcoma virus to cause sarcomas in the avian embryo. *Nature* 1984, 309:552-556
11. Dolberg DS, Hollingsworth R, Hertle M, Bissell MJ: Wounding and its role in RSV-mediated tumor formation. *Science* 1985, 230:676-678
12. Kulesa PM, Kasemeier-Kulesa JC, Teddy JM, Margaryan NV, Seftor EA, Seftor RE, Hendrix MJ: Reprogramming metastatic melanoma cells to assume a neural crest cell-like phenotype in an embryonic microenvironment. *Proc Natl Acad Sci USA* 2006, 103:3752-3757
13. Myers CA, Schmidhauser C, Mellentin-Michelotti J, Fragoso G, Roskelley CD, Casperson G, Mossi R, Pujuguet P, Hager G, Bissell MJ: Characterization of BCE-1, a transcriptional enhancer regulated by prolactin and extracellular matrix and modulated by the state of histone acetylation. *Mol Cell Biol* 1998, 18:2184-2195
14. Plachot C, Lelievre SA: DNA methylation control of tissue polarity and cellular differentiation in the mammary epithelium. *Exp Cell Res* 2004, 298:122-132
15. Pujuguet P, Simian M, Liaw J, Timpl R, Werb Z, Bissell MJ: Nidogen-1 regulates laminin-1-dependent mammary-specific gene expression. *J Cell Sci* 2000, 113:849-858
16. Debnath J, Muthuswamy SK, Brugge JS: Morphogenesis and oncogenesis of MCF-10A mammary epithelial acini grown in three-dimensional basement membrane cultures. *Methods* 2003, 30:256-268
17. Liu H, Radisky DC, Wang F, Bissell MJ: Polarity and proliferation are controlled by distinct signaling pathways downstream of PI3-kinase in breast epithelial tumor cells. *J Cell Biol* 2004, 164:603-612
18. Briand P, Nielsen KV, Madsen MW, Petersen OW: Trisomy 7p and malignant transformation of human breast epithelial cells following epidermal growth factor withdrawal. *Cancer Res* 1996, 56:2039-2044
19. Walsh DA, Perkins JP, Krebs EG: An adenosine 3',5'-monophosphate-dependant protein kinase from rabbit skeletal muscle. *J Biol Chem* 1968, 243:3763-3765
20. Ashall F, Sullivan N, Puck TT: Specificity of the cAMP-induced gene exposure reaction in CHO cells. *Proc Natl Acad Sci USA* 1988, 85:3908-3912
21. Schonberg S, Patterson D, Puck TT: Resistance of Chinese hamster ovary cell chromatin to endonuclease digestion. I. Reversal by cAMP. *Exp Cell Res* 1983, 145:57-62
22. Kim S, Harris M, Varner JA: Regulation of integrin alpha vbeta 3-mediated endothelial cell migration and angiogenesis by integrin alpha5beta1 and protein kinase A. *J Biol Chem* 2000, 275:33920-33928

23. Kawasaki H, Springett GM, Mochizuki N, Toki S, Nakaya M, Matsuda M, Housman DE, Graybiel AM: A family of cAMP-binding proteins that directly activate Rap1. *Science* 1998, 282:2275–2279
24. de Rooij J, Zwartkruis FJ, Verheijen MH, Cool RH, Nijman SM, Wittinghofer A, Bos JL: Epac is a Rap1 guanine-nucleotide-exchange factor directly activated by cyclic AMP. *Nature* 1998, 396:474–477
25. Christensen AE, Selheim F, de Rooij J, Dremier S, Schwede F, Dao KK, Martinez A, Maenhaut C, Bos JL, Genieser HG, Døskeland SO: cAMP analog mapping of Epac1 and cAMP kinase. Discriminating analogs demonstrate that Epac and cAMP kinase act synergistically to promote PC-12 cell neurite extension. *J Biol Chem* 2003, 278:35394–35402
26. Kopperud R, Krakstad C, Selheim F, Døskeland SO: cAMP effector mechanisms. Novel twists for an 'old' signaling system. *FEBS Lett* 2003, 546:121–126
27. Maniotis AJ, Chen CS, Ingber DE: Demonstration of mechanical connections between integrins, cytoskeletal filaments, and nucleoplasm that stabilize nuclear structure. *Proc Natl Acad Sci USA* 1997, 94:849–854
28. Ingber DE, Tensegrity I: Cell structure and hierarchical systems biology. *J Cell Sci* 2003, 116:1157–1173
29. Roskelley CD, Bissell MJ: The dominance of the microenvironment in breast and ovarian cancer. *Semin Cancer Biol* 2002, 12:97–104
30. Lin AY, Maniotis AJ, Valyi-Nagy K, Majumdar D, Setty S, Kadkol S, Leach L, Pe'er J, Folberg R: Distinguishing fibrovascular septa from vasculogenic mimicry patterns. *Arch Pathol Lab Med* 2005, 129:884–892
31. Ioachim E, Charchanti A, Briasoulis E, Karavasilis V, Tsanou H, Arvanitis DL, Agnantis NJ, Pavlidis N: Immunohistochemical expression of extracellular matrix components tenascin, fibronectin, collagen type IV and laminin in breast cancer: their prognostic value and role in tumour invasion and progression. *Eur J Cancer* 2002, 38:2362–2370
32. Ioachim E, Michael M, Stavropoulos NE, Kitsiou E, Salmas M, Malamou-Mitsi V: A clinicopathological study of the expression of extracellular matrix components in urothelial carcinoma. *BJU Int* 2005, 95:655–659
33. George EL, Baldwin HS, Hynes RO: Fibronectins are essential for heart and blood vessel morphogenesis but are dispensable for initial specification of precursor cells. *Blood* 1997, 90:3073–3081
34. George EL, Georges-Labouesse EN, Patel-King RS, Rayburn H, Hynes RO: Defects in mesoderm, neural tube and vascular development in mouse embryos lacking fibronectin. *Development* 1993, 119:1079–1091
35. Schor SL, Schor AM, Grey AM, Rushton G: Foetal and cancer patient fibroblasts produce an autocrine migration-stimulating factor not made by normal adult cells. *J Cell Sci* 1988, 90:391–399
36. Schor SL, Haggie JA, Durning P, Howell A, Smith L, Sellwood RA, Crowther D: Occurrence of a fetal fibroblast phenotype in familial breast cancer. *Int J Cancer* 1986, 37:831–836
37. Castellani P, Viale G, Dorcaratto A, Nicolo G, Kaczmarek J, Querze G, Zardi L: The fibronectin isoform containing the ED-B oncofetal domain: a marker of angiogenesis. *Int J Cancer* 1994, 59:612–618
38. Kaczmarek J, Castellani P, Nicolo G, Spina B, Allemanni G, Zardi L: Distribution of oncofetal fibronectin isoforms in normal, hyperplastic and neoplastic human breast tissues. *Int J Cancer* 1994, 59:11–16
39. Labat-Robert J: Thirty years after fibronectin discovery: role in malignant transformation and in ageing. *J Soc Biol* 2004, 198:287–291
40. Midulla M, Verma R, Pignatelli M, Ritter MA, Courtenay-Luck NS, George AJ: Source of oncofetal ED-B-containing fibronectin: implications of production by both tumor and endothelial cells. *Cancer Res* 2000, 60:164–169
41. Zardi L, Carnemolla B, Siri A, Petersen TE, Paoletta G, Sebastio G, Baralle FE: Transformed human cells produce a new fibronectin isoform by preferential alternative splicing of a previously unobserved exon. *EMBO J* 1987, 6:2337–2342
42. Picardo M, Schor SL, Grey AM, Howell A, Laidlaw I, Redford J, Schor AM: Migration stimulating activity in serum of breast cancer patients. *Lancet* 1991, 337:130–133
43. Durning P, Schor SL, Sellwood RA: Fibroblasts from patients with breast cancer show abnormal migratory behaviour in vitro. *Lancet* 1984, 2:890–892
44. Schor SL, Ellis IR, Jones SJ, Baillie R, Seneviratne K, Clausen J, Motegi K, Vojtesek B, Kankova K, Furrie E, Sales MJ, Schor AM, Kay RA: Migration-stimulating factor: a genetically truncated onco-fetal fibronectin isoform expressed by carcinoma and tumor-associated stromal cells. *Cancer Res* 2003, 63:8827–8836